CLNS 93/1249
CLEO 93-18

Measurements of Exclusive Semileptonic Decays of D Mesons

A. Bean,[1] J. Gronberg,[1] R. Kutschke,[1] S. Menary,[1] R.J. Morrison,[1] S. Nakanishi,[1] H.N. Nelson,[1] T.K. Nelson,[1] J.D. Richman,[1] A. Ryd,[1] H. Tajima,[1] D. Schmidt,[1] D. Sperka,[1] M.S. Witherell,[1] M. Procario,[2] S. Yang,[2] R. Balest,[3] K. Cho,[3] M. Daoudi,[3] W.T. Ford,[3] D.R. Johnson,[3] K. Lingel,[3] M. Lohner,[3] P. Rankin,[3] J.G. Smith,[3] J.P. Alexander,[4] C. Bebek,[4] K. Berkelman,[4] D. Besson,[4] T.E. Browder,[4] D.G. Cassel,[4] H.A. Cho,[4] D.M. Coffman,[4] P.S. Drell,[4] R. Ehrlich,[4] M. Garcia-Sciveres,[4] B. Geiser,[4] B. Gittelman,[4] S.W. Gray,[4] D.L. Hartill,[4] B.K. Heltsley,[4] C.D. Jones,[4] S.L. Jones,[4] J. Kandaswamy,[4] N. Katayama,[4] P.C. Kim,[4] D.L. Kreinick,[4] G.S. Ludwig,[4] J. Masui,[4] J. Mevissen,[4] N.B. Mistry,[4] C.R. Ng,[4] E. Nordberg,[4] M. Ogg,[4*] J.R. Patterson,[4] D. Peterson,[4] D. Riley,[4] S. Salman,[4] M. Sapper,[4] H. Worden,[4] F. Würthwein,[4] P. Avery,[5] A. Freyberger,[5] J. Rodriguez,[5] R. Stephens,[5] J. Yelton,[5] D. Cinabro,[6] S. Henderson,[6] K. Kinoshita,[6] T. Liu,[6] M. Saulnier,[6] F. Shen,[6] R. Wilson,[6] H. Yamamoto,[6] B. Ong,[7] M. Selen,[7] A.J. Sadoff,[8] R. Ammar,[9] S. Ball,[9] P. Baringer,[9] D. Coppage,[9] N. Copty,[9] R. Davis,[9] N. Hancock,[9] M. Kelly,[9] N. Kwak,[9] H. Lam,[9] Y. Kubota,[10] M. Lattery,[10] J.K. Nelson,[10] S. Patton,[10] D. Perticone,[10] R. Poling,[10] V. Savinov,[10] S. Schrenk,[10] R. Wang,[10] M.S. Alam,[11] I.J. Kim,[11] B. Nemati,[11] J.J. O'Neill,[11] H. Severini,[11] C.R. Sun,[11] M.M. Zoeller,[11] G. Crawford,[12] C. M. Daubenmier,[12] R. Fulton,[12] D. Fujino,[12] K.K. Gan,[12] K. Honscheid,[12] H. Kagan,[12] R. Kass,[12] J. Lee,[12] R. Malchow,[12] F. Morrow,[12] Y. Skovpen,[12†] M. Sung,[12] C. White,[12] J. Whitmore,[12] P. Wilson,[12] F. Butler,[13] X. Fu,[13] G. Kalbfleisch,[13] M. Lambrecht,[13] W.R. Ross,[13] P. Skubic,[13] J. Snow,[13] P.L. Wang,[13] M. Wood,[13] D. Bortoletto,[14] D.N. Brown,[14] J. Fast,[14] R.L. McIlwain,[14] T. Miao,[14] D.H. Miller,[14] M. Modesitt,[14] S.F. Schaffner,[14] E.I. Shibata,[14] I.P.J. Shipsey,[14] P.N. Wang,[14] M. Battle,[15] J. Ernst,[15] H. Kroha,[15] Y. Kwon,[15] S. Roberts,[15] K. Sparks,[15] E.H. Thorndike,[15] C.H. Wang,[15] J. Dominick,[16] S. Sanghera,[16] V. Shelkov,[16] T. Skwarnicki,[16] R. Stroynowski,[16] I. Volobouev,[16] P. Zadorozhny,[16] M. Artuso,[17] D. He,[17] M. Goldberg,[17] N. Horwitz,[17] R. Kennett,[17] G.C. Moneti,[17] F. Muheim,[17] Y. Mukhin,[17] S. Playfer,[17] Y. Rozen,[17] S. Stone,[17] M. Thulasidas,[17] G. Vasseur,[17] G. Zhu,[17] J. Bartelt,[18] S.E. Csorna,[18] Z. Egyed,[18] V. Jain,[18] D.S. Akerib,[19] B. Barish,[19] M. Chadha,[19] S. Chan,[19] D.F. Cowen,[19] G. Eigen,[19] J.S. Miller,[19] C. O'Grady,[19] J. Urheim,[19] A.J. Weinstein,[19] D. Acosta,[20] M. Athanas,[20] G. Masek,[20] and H. Paar[20]

(CLEO Collaboration)

[1] *University of California, Santa Barbara, California 93106*
[2] *Carnegie-Mellon University, Pittsburgh, Pennsylvania 15213*
[3] *University of Colorado, Boulder, Colorado 80309-0390*
[4] *Cornell University, Ithaca, New York 14853*
[5] *University of Florida, Gainesville, Florida 32611*
[6] *Harvard University, Cambridge, Massachusetts 02138*
[7] *University of Illinois, Champaign-Urbana, Illinois, 61801*
[8] *Ithaca College, Ithaca, New York 14850*
[9] *University of Kansas, Lawrence, Kansas 66045*
[10] *University of Minnesota, Minneapolis, Minnesota 55455*
[11] *State University of New York at Albany, Albany, New York 12222*
[12] *Ohio State University, Columbus, Ohio, 43210*
[13] *University of Oklahoma, Norman, Oklahoma 73019*
[14] *Purdue University, West Lafayette, Indiana 47907*
[15] *University of Rochester, Rochester, New York 14627*
[16] *Southern Methodist University, Dallas, Texas 75275*
[17] *Syracuse University, Syracuse, New York 13244*
[18] *Vanderbilt University, Nashville, Tennessee 37235*
[19] *California Institute of Technology, Pasadena, California 91125*
[20] *University of California, San Diego, La Jolla, California 92093*

Abstract

Using a sample of integrated luminosity 1.68 fb^{-1} collected with the CLEO-II detector at the Cornell Electron Storage Ring, we measure the branching ratios for the dominant exclusive semileptonic decays $D \to K\ell\nu$ and $D \to K^*\ell\nu$, using charged and neutral D mesons. We also make a precise measurement of the vector form factor for the decay $D^0 \to K^-\ell^+\nu$, using a sample of 2700 events.

Typeset using REVTEX

*Permanent address: Carleton University, Ottawa, Canada K1S 5B6

†Permanent address: INP, Novosibirsk, Russia

The decays $D \to K\ell\nu$ and $D \to K^*\ell\nu$ provide a good environment in which to test theoretical understanding of form factors for heavy quark decay. The Cabibbo-Kobayashi-Maskawa (CKM) matrix element $|V_{cs}|$ is known from unitarity, so one can make an absolute measurement of the form factors and compare them with theoretical models. In addition, it is important to determine whether the decays to pseudoscalar and vector mesons saturate the inclusive semileptonic decay rate. Finally, using Heavy Quark Effective Theory (HQET) [1] or lattice gauge techniques, the measured charm form factors can be related to those needed to interpret both $b \to u$ exclusive decays and rare B decays involving Flavor Changing Neutral Currents (FCNC) [2].

In this paper, we report a study of the decay modes $D \to K\ell\nu$ and $D \to K^*\ell\nu$, using charged and neutral D mesons. The analysis uses a sample of over 2 million $e^+e^- \to c\,\overline{c}$ events collected with the CLEO-II detector [3] at the Cornell Electron Storage Ring (CESR). The integrated luminosity was 1.18 fb^{-1} at the $\Upsilon(4S)$ energy of 10.58 GeV and 0.50 fb^{-1} in the continuum just below the resonance.

We use the decays $D^{*+} \to \pi_s^+ D^0$ to tag D^0 mesons and $D^{*+} \to \pi_s^0 D^+$ to tag D^+ mesons, where π_s refers to the slow pion. Cuts on the unique kinematics of the π_s in the D^* decay reduce backgrounds considerably. We describe the analysis of the $D^0 \to K^-\ell^+\nu$ decay in detail, using it as a prototype for the four separate analyses. Throughout this paper, charge conjugate modes are implied. In describing the other analyses, we will point out variations from the basic method.

In the familiar use of the decay $D^{*+} \to \pi_s^+ D^0$ to obtain clean samples of hadronic decays such as $D^0 \to K^-\pi^+$, one exploits the narrow peak in the $m_{K^-\pi^+\pi_s^+} - m_{K^-\pi^+}$ spectrum at the $D^{*+} - D^0$ mass difference of 145.4 MeV. The present analysis takes advantage of a similar effect in $D^0 \to K^-\ell^+\nu$ events, although in the semileptonic decay the undetected neutrino broadens the peak substantially. Figure 1 shows the mass difference $\delta m = m_{K\ell\pi} - m_{K\ell}$ vs the $K\ell$ mass $m_{K\ell}$ for a Monte Carlo sample of $D^0 \to K^-\ell^+\nu$ decays.

We first select events containing a possible $K^-\ell^+\pi_s^+$ combination. Because of the small statistical error achievable, the selection criteria are chosen to minimize systematic errors.

To reduce the background from B decays, we require $R_2 = H_2/H_0 > 0.2$ where R_2 is a ratio of Fox-Wolfram event shape variables [4]. All tracks are required to come from the region of the event vertex. Electrons are identified using a likelihood function which incorporates information from the calorimeter and dE/dx systems and muons are identified by their ability to penetrate an iron absorber and reach detection planes at a depth of at least five nuclear absorption lengths [3]. We only use leptons from kinematic regions in which the efficiency is well understood; leptons are required to have $|\cos\theta| < 0.81$, where θ is the angle of the lepton momentum with the beam line. The minimum momentum is 0.7 GeV/c for electrons and 1.4 GeV/c for muons, except for $|\cos\theta| > 0.61$, where the minimum muon momentum is 1.9 GeV/c. We require that the time-of-flight and dE/dx information for the kaon be consistent with the expected values, but not that other identifications be ruled out. The maximum allowed momentum for the slow pion is 0.5 GeV/c, and the minimum momentum for the kaon is 0.5 GeV/c. Finally, we apply a minimum momentum cut for the $K - \ell$ system of 1.8 GeV/c, because the backgrounds increase at lower momentum. This corresponds approximately to a lower limit of 2.4 GeV/c on the D^{*+} momentum; thus the charm signal events observed are predominantly from directly produced charm, and not from B decays.

The remaining event sample contains mostly signal. We fit the δm spectrum to obtain the number of signal events. We make use of the correlation shown in Figure 1 between the width of the signal in δm and $m_{K\ell}$ by splitting the data into two mass bins: (a)$1.2 < m_{K\ell} < 1.4$ GeV/c^2, and (b)$1.4 < m_{K\ell} < 1.8$ GeV/c^2. We do not use muons in the low mass sample, because they are predominantly near the minimum energy accepted, where the efficiency and hadron fake rate are less precisely known. Muons account for about 40% of the events in the high mass sample.

Figure 2 shows the δm spectra for the (a) low mass($m_{K\ell}$) and (b) high mass data samples. The function used in the fit to the spectra is $n(\delta m) = N_K f_K + N_{K^*} f_{K^*} + N_\pi f_\pi + N_{fake} f_{fake} + N_b f_b$, where the subscripts denote: K =signal, K^* =feeddown from $D^0 \to K^* \ell\nu$ decays, π =feeddown from $D^0 \to \pi\ell\nu$ decays, fake= D^0 hadronic decays with one track misidentified as a lepton, and b = other backgrounds. The f_i represent normalized shapes which are taken from Monte Carlo samples (K, K^*, π) or from the data (fake, b). The terms N_K and N_b float in the fit, while the other N_i terms are fixed using the measured branching fractions and efficiencies from Monte Carlo studies. The rate for $D \to \pi\ell\nu$ is assumed to be $13 \pm 3\%$ of the measured $D \to K\ell\nu$ rate. The shape f_b is taken from data with a slow pion of the wrong sign and describes all backgrounds not explicitly handled elsewhere in the fit. Checks of all of the major components of the background show that the wrong sign gives a good representation of the smooth background shape f_b. The number of events in each feedthrough mode and the results of the fit are shown in Table I. We find 906 ± 38 and 1604 ± 47 events in the low mass and high mass samples, respectively.

For each region of $m_{K\ell}$, we calculate the yield of produced events by dividing the number of observed events by the efficiency as determined by Monte Carlo simulation. The efficiencies in table 1 are defined as the fraction of all semileptonic decays (electrons and muons) that are accepted. The high mass yield has been corrected upward by 1.2% to take into account that the muon decay rate is 3% less than that for electrons [5]. The yields obtained are $N_{low} = 46200 \pm 1900 \pm 2400$ and $N_{high} = 45600 \pm 1300 \pm 2000$. We take a weighted average of the high and low mass numbers, taking into account common errors, and correct it upward by 1.6% because of efficiency loss due to final state radiation in the decay $Ke\nu$ which is not simulated in the Monte Carlo [6]. Finally, we divide by two, for the two types of leptons, to get the number of $D^0 \to K^- e^+ \nu$ events produced in the full data sample of $23290 \pm 550 \pm 980$. Because of the muon correction noted above, the yield and the branching ratios derived from it are for the decay into electrons. The second error on the yield is systematic, and includes Monte Carlo statistics (1.2%); uncertainties in the number of lepton fakes (0.8%), K^* decays (1%), and π decays (2%); variations in the form factor shape (1%) and in background shapes (1.8%); and the uncertainty in the lepton identification efficiency (2.5%). We find good agreement between the yields from the electron and muon samples when analyzed separately, with a 9% statistical error due to the smaller muon sample.

We measure the ratio $R_0 = \frac{B(D^0 \to K^- e^+ \nu)}{B(D^0 \to K^- \pi^+)}$. By normalizing to this mode, and choosing cuts on the hadronic mode which match those for the semileptonic mode, we insure that the systematic errors on all reconstruction efficiencies almost cancel. Thus the only important efficiency error is that for lepton identification. The number of $D^{*+} \to \pi_s^+ D^0, D^0 \to K^- \pi^+$ events observed with similar cuts is 5787 ± 86, and the efficiency determined using Monte Carlo simulation is $(24.3 \pm 0.3)\%$. The number produced in the normalization mode is therefore $23810 \pm 350 \pm 360$. From these two numbers we calculate the ratio R_0 of branching fractions, which is shown in Table II. Using the CLEO measurement $B(D^0 \to K^- \pi^+) = (3.91 \pm 0.08 \pm 0.17)\%$ [7], we calculate $B(D^0 \to K^- e^+ \nu) = (3.82 \pm 0.11 \pm 0.25)\%$.

The analysis for the mode $D^{*+} \to \pi_s^0 D^+, D^+ \to \overline{K}^0 \ell^+ \nu$ is similar to the one just described. The $\overline{K^0}$ is observed using the decay $K_S^0 \to \pi^+ \pi^-$. We require that the neutral slow pion momentum be greater than 180 MeV/c and the K_S^0 momentum be greater than 0.5 GeV/c. We also require that the pions from the K_S^0 decay make a good vertex well separated from the interaction point. In this analysis, and in the two analyses of decays to $K^* \ell \nu$ described below, we calculate the transverse momentum of the $K\ell$ system relative to the thrust axis of the event and require that $p_t < 1.0$ GeV/c. This cut reduces the background from random $K - \ell$ combinations. Figure 2 shows the δm spectra for the (c) low mass and (d) high mass samples. The function used to fit the data is $n(\delta m) = N_K f_K + N_{K^*} f_{K^*} + N_{fake} f_{fake} + N_b f_b$, where the f_{fake} has the same shape as the signal. The K^* term includes the two processes $D^{*+} \to \pi_s^0 D^+, D^+ \to K_S^0 \pi^0 \ell^+ \nu$ and $D^{*0} \to \pi_s^0 D^0, D^0 \to K_S^0 \pi^- \ell^+ \nu$. The function f_b is taken from the π_s^0 sideband region. The results from the fits are shown in Table I.

The method of calculating the number of observed events is the same as described above. Taking the weighted average, dividing by two for the two lepton flavors, and correcting for the $\overline{K^0} \to \pi^+ \pi^-$ branching fraction, we find the measured number of signal events to be $28300 \pm 3100 \pm 2100$. The largest systematic errors are for background shapes, lepton identification efficiency, and Monte Carlo statistics. In the normalization mode $D^+ \to \overline{K}^0 \pi^+$, there are

230 ± 18 events observed with an efficiency of 6.15%. Thus the yield for the normalization mode after correcting for the $\overline{K^0} \to \pi^+\pi^-$ branching fraction is $10900 \pm 850 \pm 730$. The final result is the value of $R_+ = \frac{B(D^+ \to \overline{K^0} e^+ \nu)}{B(D^+ \to \overline{K}^0 \pi^+)}$ shown in Table II.

We analyze the two decay modes $D \to K^* \ell \nu$ using the process $K^* \to K\pi_F$. (We call this pion the fast pion π_F to distinguish it from the slow pion produced in the D^{*+} decay.) For the $D^0 \to K^{*-}\ell^+\nu$ mode, we use the decay $K^{*-} \to K^0_S \pi^-_F$ and the normalization mode $D^0 \to \overline{K^0}\pi^+\pi^-$. The fourth mode studied is $D^+ \to \overline{K}^{*0}\ell^+\nu$, for which we use the decay $\overline{K^{*0}} \to K^-\pi^+_F$ and normalization mode $D^+ \to K^-\pi^+\pi^+$. These analyses have the extra complication that most of the backgrounds are from random $K\pi_F$ combinations. We follow the procedure as outlined above of fitting the δm spectrum, except that the contents of each bin in the δm plot is obtained from a fit to the $K\pi$ mass spectrum to extract the K^* component. The error on the number of events in each bin is taken from this fit. We require the $K\pi_F$ system to have a momentum greater than 0.7 GeV/c, the $K\pi_F\ell$ system to have a momentum greater than 2.0 GeV/c, and $p_t < 1.0$ GeV/c. For the $D^+ \to \overline{K}^{*0}\ell^+\nu$ mode, the cuts are the same as for $D^0 \to K^{*-}\ell^+\nu$, except that the slow pion requirements are those used for the $D^+ \to \overline{K}^0\ell^+\nu$ analysis.

After fitting the $K\pi$ mass spectrum to determine the number of K^* events in each δm bin, we obtain the distributions shown in Figure 3. In the background regions of the δm plot, the number of $K\pi_F$ combinations in the K^* mass region before fitting is typically 5 times the K^* component which is shown in Figure 3. In the δm signal region the signal to background ratio is 2 to 1. The feedthrough from $D \to K^*\pi\ell\nu$ is negligible, based on existing limits on the branching ratio [8]. The results of the fits and the efficiencies are shown in Table III. The phase space correction is 5% for muons, which causes a 1.6% correction to the yields of the high mass sample. The correction for final state radiation is 0.9%. The yield of produced $D^0 \to K^{*-}e^+\nu$ events after correcting for the $K^* \to K\pi$ and $\overline{K^0} \to \pi^+\pi^-$ branching fractions is $13800 \pm 2000 \pm 900$, and for the normalization mode $D^0 \to K^0_S\pi^+\pi^-$, it is $36300 \pm 1200 \pm 1600$. The largest systematic errors are for the Monte Carlo statistics, the model dependence, the uncertainty in fitting shapes, and the uncertainty in the lepton identification efficiency. The ratio $R_0^* = \frac{B(D^0 \to K^{*-} e^+ \nu)}{B(D^0 \to \overline{K^0} \pi^+ \pi^-)}$ extracted from these numbers is given in Table II.

The δm distributions for the $D^+ \to \overline{K^{*0}} \ell^+ \nu$ mode are also shown in Figure 3, and the results of the fits are in Table III. The yield of produced events after correcting for the $K^* \to K\pi$ branching fraction for the signal mode is $18000 \pm 1600 \pm 1700$ and for the normalization mode is $27000 \pm 2500 \pm 1000$. In addition to the systematic errors that apply for $D^0 \to K^{*-} e^+ \nu$, there is a 7% systematic error on the uncertainty in the subtraction of π^0 sidebands, which is the largest systematic error. The ratio $R_+^* = \frac{B(D^+ \to \overline{K^{*0}} e^+ \nu)}{B(D^+ \to K^- \pi^+ \pi^+)}$ is also shown in Table II.

Using the large $D^0 \to K^- \ell^+ \nu$ sample, we are able to measure the single vector form factor. The differential decay rate for $D \to \overline{K} \ell^+ \nu$ has a simple dependence on this form factor:

$$\frac{d\Gamma}{dq^2} = \frac{G_F^2 |V_{cs}|^2 P_K^3}{24\pi^3} |f_+(q^2)|^2, \tag{1}$$

where $q^2 = M_D^2 + M_K^2 - 2M_D E_K$ is the square of the lepton-neutrino mass, E_K is the energy of the kaon in the D rest frame, and $P_K = \sqrt{E_K^2 - M_K^2}$ is the momentum of the kaon in that frame. The form factor represents a measure of the overlap of the D and K wave functions. The maximum value of $f_+(q^2)$ occurs at q_m^2, the maximum value of q^2, which corresponds to the K being at rest in the D rest frame. The q^2 dependence is parameterized either with an exponential form factor, $f_+(q^2) = f_+(q_m^2) \times e^{-\alpha(q_m^2 - q^2)} = f_+(0) e^{\alpha q^2}$ [9], or with a pole form $f_+(q^2) = \frac{f_+(0)}{1 - q^2/m_p^2}$ [10]. These two forms are practically indistinguishable over the accessible q^2 range in D decay, and the two constants are related by $\alpha = 1/(m_p^2 - q_{ave}^2)$, where q_{ave} is the mean value of the q^2 distribution. In the ISGW model [9], $\alpha = 0.21$ GeV^{-2}. In other models [10] that use the pole form, the pole mass is taken to be 2.1 GeV, the D_s^{*+} mass, which corresponds to $\alpha = 0.25$ GeV^{-2}.

We can use the measured value of $B(D^0 \to K^- \ell^+ \nu)$ quoted above and the world average for the D^0 lifetime, (0.420 ± 0.008)ps [11] to obtain the decay width $\Gamma(D^0 \to K^- e^+ \nu) = (9.1 \pm 0.3 \pm 0.6) \times 10^{10} s^{-1}$. We integrate this differential decay rate using the form $e^{\alpha q^2}$ with the measured value of α (see below) to convert this to a value of the form factor at $q^2 = 0$, and obtain $f_+(0) = 0.77 \pm 0.01 \pm 0.04$. This value agrees well with quark models [9,10,12] and lattice gauge calculations [13,14].

To measure the shape parameter α, we fit the q^2 distribution. We determine q^2 using the formula $q^2 = M_\ell^2 + 2[E_\ell E_\nu - P_\ell P_\nu \cos\theta_{\ell\nu}]$, working in the $K\ell$ rest frame. All these quantities are well measured except $\theta_{\ell\nu}$, the angle between the lepton and the neutrino. We can limit the range for this angle, however, using other measured angles. The angle between the lepton and the pion in the $K\ell$ frame, $\theta_{\pi\ell}$, is measured directly, and the angle between the neutrino and the pion $\theta_{\pi\nu}$ can be derived from δm and $m_{K\ell}$. The range for the lepton-neutrino angle is therefore bounded by the values $\cos\theta_{\ell\nu} = \cos\theta_{\pi\nu}\cos\theta_{\pi\ell} \pm \sin\theta_{\pi\nu}\sin\theta_{\pi\ell}$. We choose the most likely value of q^2 interpolated between these limits using a simple parameterization of the known decay angular distribution. The resulting resolution on q^2 is 0.24 GeV^2 (rms).

Figure 4 shows the measured q^2 distribution for events satisfying the $D^0 \to K^-\ell^+\nu$ cuts and having $\delta m < 0.150 + 0.04 \times (1.8 - m_{K\ell})$. We make a fit of the spectrum to a function of the form $dN/dq^2 = [N_K\ g_K + N_\pi\ g_\pi]\ e^{2\eta q^2} + N_{K^*}\ g_{K^*} + N_{fake}\ g_{fake} + N_b\ g_b$. Here the parameter η represents the difference in the exponential shape parameter in the data from that used for the Monte Carlo, $\alpha_0 = 0.21\ \mathrm{GeV}^{-2}$. $N_K = 2700$ is the number of $D^0 \to K^-\ell^+\nu$ events, $N_\pi = 230$ are from $D^0 \to \pi^-\ell^+\nu$ with a similar distribution, $N_{K^*} = 146$ are from $D^0 \to K^{*-}\ell^+\nu$, $N_{fake} = 70$ are from fake leptons, and $N_b = 305$ are from other background sources. All of the normalized functions $g_i(q^2)$ are determined from the Monte Carlo, except g_{fake} which is determined from data and g_b which is determined from wrong sign events, and checked with other background samples.

The method by which we choose the value of q^2 depends slightly on the form factor shape used in the Monte Carlo, so one has to make sure that this does not cause a bias in the final result. We test this by constructing simulated data samples with different shapes from that used in the standard Monte Carlo. We find that if the test data are generated with a value of α, our fit gives $\eta = 0.7(\alpha - \alpha_0)$. Thus we can extract the true value of α without bias, and the sensitivity is not degraded too much by the smearing in measuring q^2.

The resulting value from the fit is $\eta = 0.054 \pm 0.030$, corresponding to a slope parameter of $\alpha = 0.29 \pm 0.04 \pm 0.06$ GeV^{-2}. The major systematic errors are in the shapes of the functions used for signal and Monte Carlo. In the ISGW model, this value of α corresponds to a measurement of their parameter $\kappa = 0.57 \pm 0.07$, assuming the meson sizes and quark masses are precisely known, compared to the value of 0.7 they estimate. Given the uncertainties in the quark masses, this represents reasonable agreement with the original choice for that parameter. If instead we interpret this as a pole mass, this corresponds to a value of $m_p = 2.00 \pm 0.12 \pm 0.18$ GeV, which agrees with the single D_s^* pole. This measurement is consistent with previous published results [15], but is significantly more precise.

In conclusion, we have measured all four of the charm semileptonic branching fractions $D \to K(K^*)\ell^+\nu$ in one experiment. The relative branching ratio for $D^0 \to K^-\ell^+\nu$ shown in Table II has a 5% error. We have made a precise measurement of the vector form factor $f_+(q^2)$, both the normalization and shape. The relative branching ratios for the other three modes are measured with total errors of $15 - 20\%$.

The yields for the four semileptonic decays can be used to calculate the ratio of $\frac{\Gamma(D \to K^* e\nu)}{\Gamma(D \to K\ e\nu)}$. The result for the D^0 is $\frac{\Gamma(D^0 \to K^{*-}e^+\nu)}{\Gamma(D^0 \to K^-e^+\nu)} = 0.60 \pm 0.09 \pm 0.07$; for the D^+ it is $\frac{\Gamma(D^+ \to \overline{K^{*0}}e^+\nu)}{\Gamma(D^+ \to \overline{K^0}e^+\nu)} = 0.65 \pm 0.09 \pm 0.10$. Note that these ratios are calculated directly from the yields of the four semileptonic modes, without using any hadronic modes for normalization. Assuming the equality of semileptonic rates for the two mesons, we can average the two ratios, to get our best value,

$$\frac{\Gamma(D \to K^* e\ \nu)}{\Gamma(D \to K\ e\ \nu)} = 0.62 \pm 0.08. \tag{2}$$

With better errors, this value confirms the result seen in earlier experiments [11] that this ratio is significantly less than the range of 0.9-1.2 predicted by quark models [9,12,10] and lattice gauge calculations [13,14].

The best value of $\Gamma(D \to K^* e\ \nu)$ is obtained by normalizing the measurements for both charge modes to $\Gamma(D^0 \to K^-\pi^+)$. Using only the yields measured in this analysis, and again assuming the equality of semileptonic rates to combine D^+ and D^0, we calculate

$\Gamma(D \to K^* e\nu)/\Gamma(D^0 \to K^-\pi^+) = (0.61 \pm 0.07)$. Multiplying this by the rate $\Gamma(D^0 \to K^-\pi^+) = (9.3 \pm 0.4) \times 10^{10} s^{-1}$, which is obtained from the CLEO measurement for the branching ratio [7] and the PDG lifetime [11], gives the value

$$\Gamma(D \to K^* e\ \nu) = (5.7 \pm 0.7) \times 10^{10} s^{-1}. \tag{3}$$

The sum of the two decay rates is $\Gamma(D \to [K + K^*]\ e\ \nu) = (14.8 \pm 1.3) \times 10^{10} s^{-1}$. The inclusive semileptonic rate is measured to be $\Gamma(D \to e\ X) = (16.7 \pm 1.5) \times 10^{10} s^{-1}$, averaging over the measured D^0 and D^+ rates [11]. Since Cabibbo-suppressed decays are expected to comprise about 8% of the inclusive semileptonic rate, the results are consistent with the decays to pseudoscalar and vector mesons saturating the inclusive rate.

We can also relate D^+ and D^0 branching fractions by taking advantage of the isospin relationship $\Gamma(D^0 \to K^- e^+ \nu) = \Gamma(D^+ \to \overline{K^0} e^+ \nu)$:

$$\frac{B(D^0 \to K^-\pi^+)}{B(D^+ \to \overline{K}^0 \pi^+)} = \frac{R_+}{R_0} \times \frac{\tau_{D^0}}{\tau_{D^+}} = 1.05 \pm 0.15 \pm 0.12. \tag{4}$$

The ratio of the two $K\pi$ modes calculated from the individual branching fractions given by the PDG fit is 1.40 ± 0.23. [11]. Our results favor a larger value for $B(D^+ \to \overline{K}^0 \pi^+)$ than the present world average.

We gratefully acknowledge the effort of the CESR staff in providing us with excellent luminosity and running conditions. This work was supported by the National Science Foundation, the U.S. Dept. of Energy, the Heisenberg Foundation, the SSC Fellowship program of TNRLC, and the A.P. Sloan Foundation.

TABLES

TABLE I. Fit results for $D \to K\ell\nu$. The number N_{fit} is the number of signal events found. The efficiency listed just includes detector acceptance. To obtain the correct yields, one must multiply the efficiency by the branching fraction (BF) given in the last column, which accounts for the $\overline{K^0}$ to decay into the $\pi^+\pi^-$ final state.

	$m_{K\ell}$	$K^*\ell\nu$	$\pi\ell\nu$	Fake	N_{fit}	$\epsilon(\%)$	BF
D^0	1.2-1.4	78 ± 16	61 ± 14	7 ± 5	906 ± 38	1.96 ± 0.04	1.0
	1.4-1.8	55 ± 11	148 ± 35	64 ± 20	1604 ± 47	3.56 ± 0.06	1.0
D^+	1.2-1.4	13 ± 4	0	1 ± 1	64 ± 14	0.33 ± 0.03	0.34
	1.4-1.8	0	0	7 ± 3	122 ± 16	0.66 ± 0.04	0.34

TABLE II. Results on semileptonic branching fractions. Each number in the third column is the ratio of the semileptonic branching fraction to the branching fraction for the hadronic normalization mode listed in the second column.

signal mode	normalization mode	ratio of BR's
$D^0 \to K^-e^+\nu$	$D^0 \to K^-\pi^+$	$R_0 = 0.978 \pm 0.027 \pm 0.044$
$D^+ \to \overline{K^0}e^+\nu$	$D^+ \to \overline{K^0}\pi^+$	$R_+ = 2.60 \pm 0.35 \pm 0.26$
$D^0 \to K^{*-}e^+\nu$	$D^0 \to \overline{K^0}\pi^+\pi^-$	$R_0^* = 0.38 \pm 0.06 \pm 0.03$
$D^+ \to \overline{K^{*0}}e^+\nu$	$D^+ \to K^-\pi^+\pi^+$	$R_+^* = 0.67 \pm 0.09 \pm 0.07$

TABLE III. Fit results for $D \to K^{*}\ell\nu$. The efficiency listed in column three includes only acceptance contributions. To obtain the correct yields, one should multiply the efficiency by the branching fraction (BF) given in the last column, which accounts for the K^{*} to decay into the $K\pi$ final state and in the D^0 case for the $\overline{K^0}$ decay into $\pi^+\pi^-$.

	$m_{K\pi\ell}$	N_{fit}	$\epsilon(\%)$	BF
D^0	1.2-1.4	55 ± 13	0.96 ± 0.06	0.23
	1.4-1.8	97 ± 18	1.46 ± 0.07	0.23
D^+	1.2-1.4	345 ± 42	1.38 ± 0.10	0.67
	1.4-1.8	365 ± 45	1.62 ± 0.09	0.67

REFERENCES

[1] N. Isgur and M.B. Wise, Phys. Rev **D42** (1989) 2388.

[2] A. Ali, C. Greub, and T. Mannel in DESY preprint 93-016 (1993), to be published in Proceedings of the ECFA Workshop on the Physics of a B Meson Factory, eds. R. Aleksan and A. Ali (1993).

[3] Y. Kubota *et al.*, Nucl. Instrum. Methods **A320**, (1992) 66.

[4] G. Fox and S. Wolfram, Phys. Rev. Lett. **41** (1978) 1581.

[5] J.G. Körner and G.A. Schuler, Z. Phys. **C46**, (1990) 93.

[6] D. Atwood and W.J. Marciano, Phys. Rev. **D41**, (1990) 1736.

[7] D. Akerib *et al.*, CLEO preprint CLEO 93-12(1993), submitted to Phys. Rev. Lett.

[8] J. Anjos *et al.* (E691), Phys. Rev. **D45**, (1992) R2177; K. Kodama *et al.* (E653), Carnegie-Mellon preprint CMU-HEP 93-14, to appear in Phys. Lett. B (1993).

[9] N. Isgur *et al.*, Phys. Rev. **D39**, (1989) 799.

[10] M. Wirbel *et al.*, Z. Phys. **C29**, (1985) 627; and J.G. Körner and G.A. Schuler, Z. Phys. **C38**, (1988) 511.

[11] K. Hikasa *et al.*, (Particle Data Group), Phys. Rev. **D45**, (1992) S1.

[12] T. Altomari and L. Wolfenstein, Phys. Rev. **D37**, (1988) 681; and F.J. Gilman and R.L. Singleton, Phys. Rev. **D41**, (1990) 142.

[13] V. Lubicz *et al.*, Phys. Lett. **B274** (1992) 415.

[14] C. Bernard *et al.*, Phys. Rev. **D43** (1991) 2140 and Phys. Rev. **D47** (1993) 998.

[15] J.C. Anjos *et al.* (E691), Phys. Rev. Lett. **62**, (1989) 1587; J. Adler *et al.* (Mark III) Phys. Rev. Lett. **62**, (1989) 1821; G. Crawford *et al.* (CLEO), Phys. Rev. **D44**, (1991)

3394; and J. Cumalat in *The Fermilab Meeting: DPF '92*, ed. Carl Albright *et al.*, (World Scientific, Singapore, 1993).

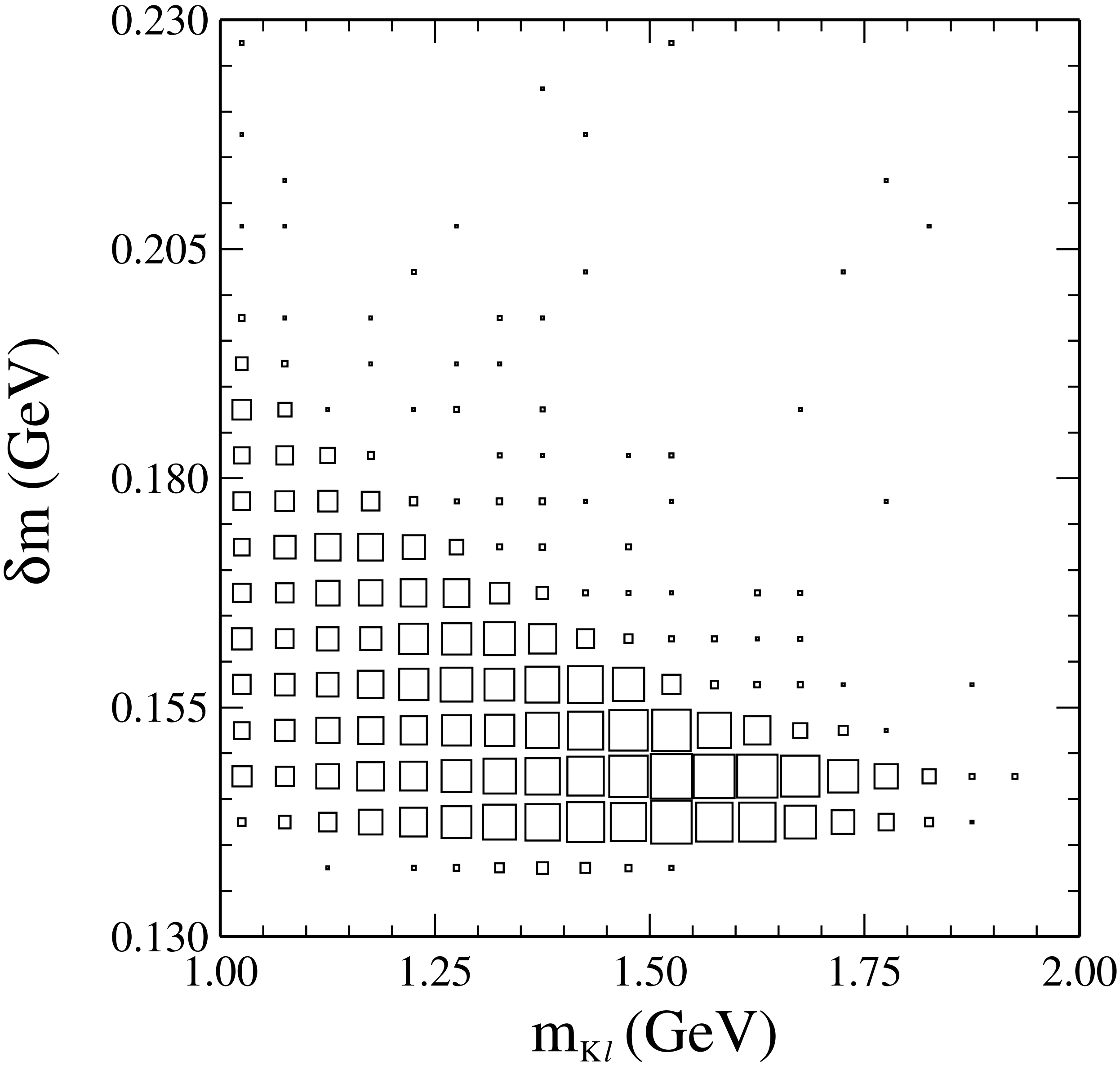

FIG. 1. A plot of $\delta m = m_{K^-\ell^+\pi_s^+} - m_{K^-\ell^+}$ versus $m_{K^-\ell^+}$ for $D^{*+} \to D^0\pi_s^+$, $D^0 \to K^-\ell^+\nu$ Monte Carlo events.

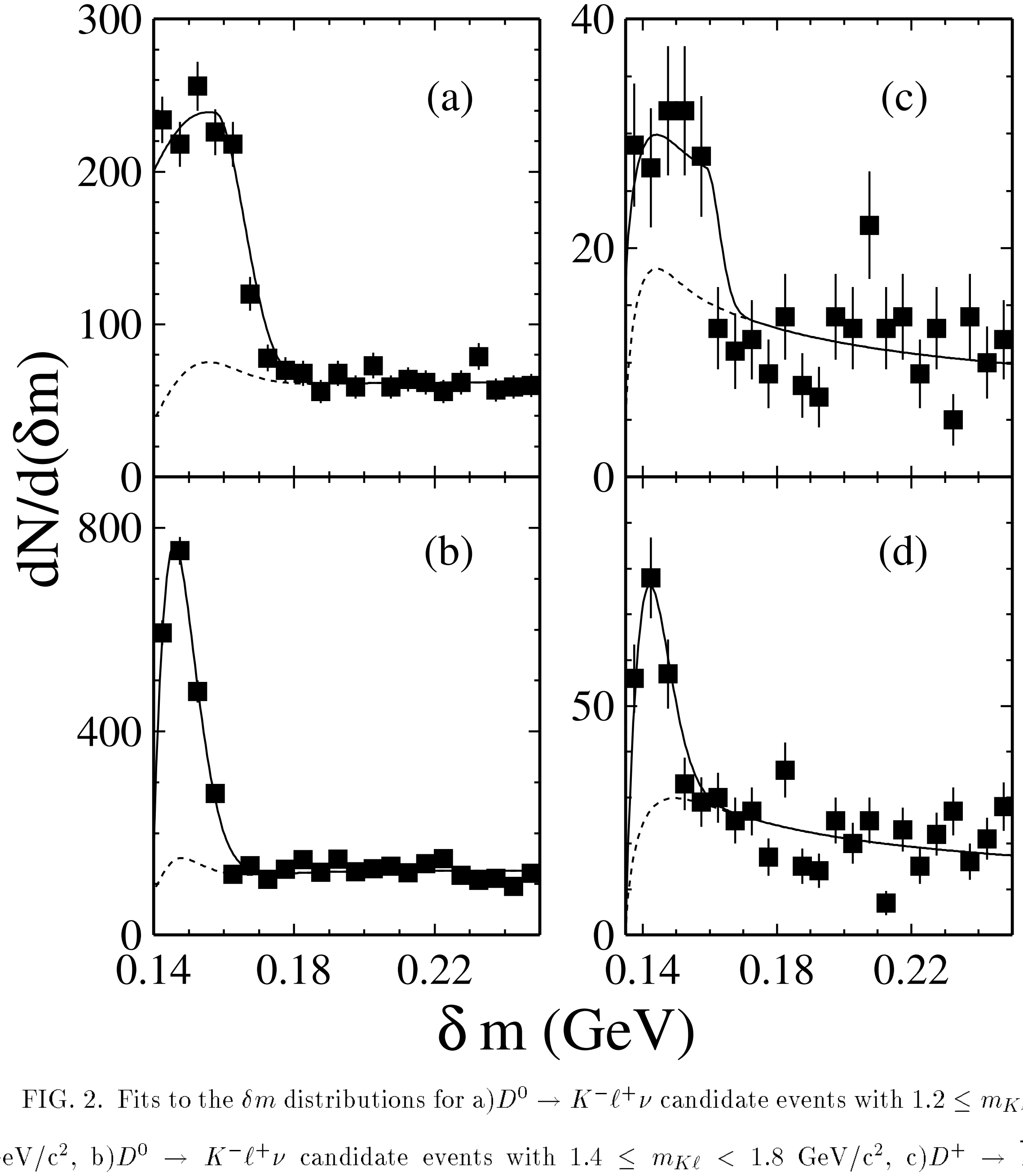

FIG. 2. Fits to the δm distributions for a)$D^0 \to K^- \ell^+ \nu$ candidate events with $1.2 \leq m_{K\ell} < 1.4$ GeV/c^2, b)$D^0 \to K^- \ell^+ \nu$ candidate events with $1.4 \leq m_{K\ell} < 1.8$ GeV/c^2, c)$D^+ \to \overline{K^0} \ell^+ \nu$ candidate events with $1.2 \leq m_{K\ell} < 1.4$ GeV/c^2, and d)$D^+ \to \overline{K^0} \ell^+ \nu$ candidate events with $1.4 \leq m_{K\ell} < 1.8$ GeV/c^2. The dashed lines indicate the sum of all backgrounds.

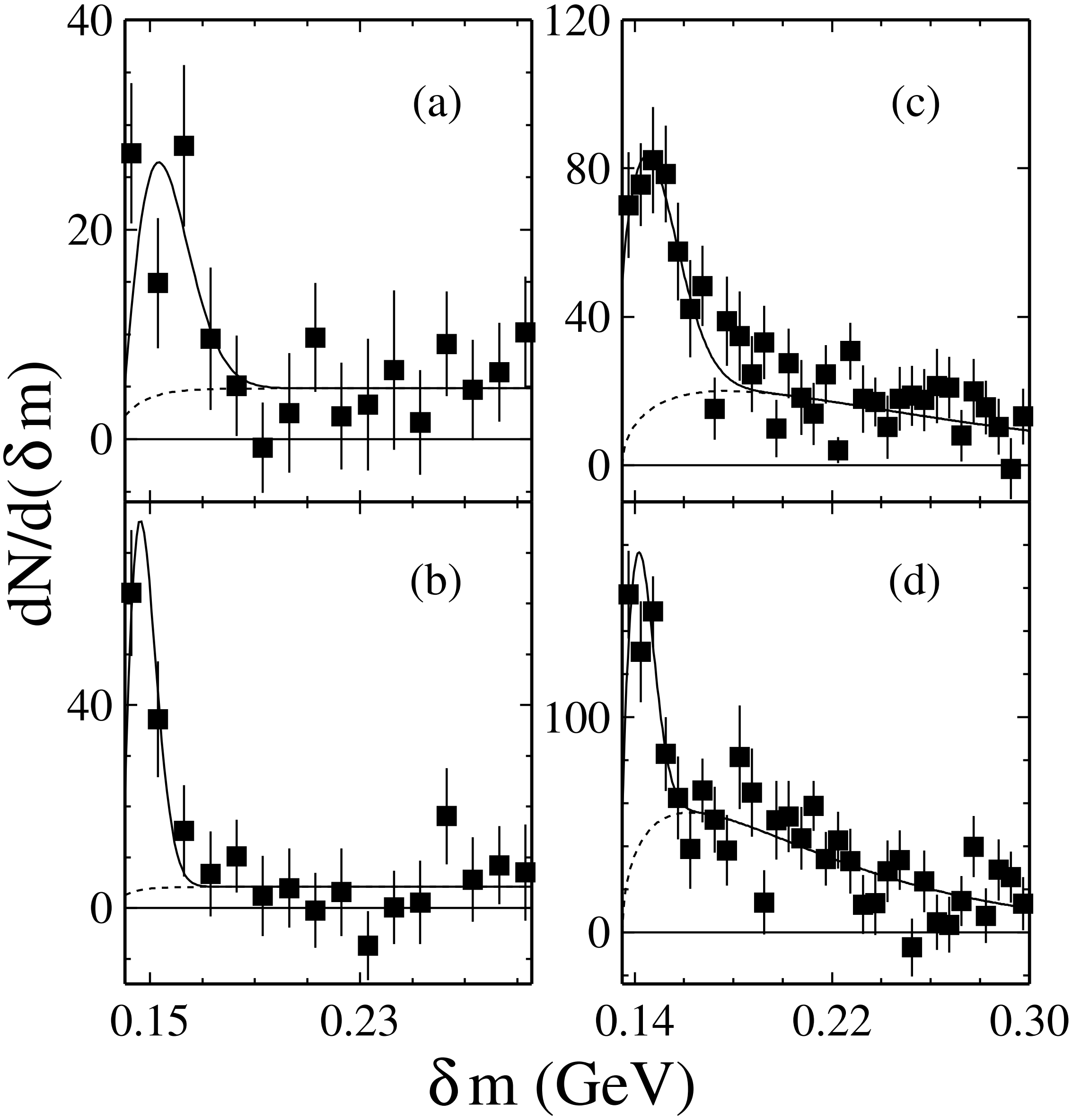

FIG. 3. Fits to the δm distributions for a)$D^0 \to K^{*-}\ell^+\nu$ candidate events with $1.2 \leq m_{K\ell} < 1.4$ GeV/c^2, b)$D^0 \to K^{*-}\ell^+\nu$ candidate events with $1.4 \leq m_{K\ell} < 1.8$ GeV/c^2, c)$D^+ \to \overline{K^{*0}}\ell^+\nu$ candidate events with $1.2 \leq m_{K\ell} < 1.4$ GeV/c^2, and d)$D^+ \to \overline{K^{*0}}\ell^+\nu$ candidate events with $1.4 \leq m_{K\ell} < 1.8$ GeV/c^2. These distributions are obtained after fitting for the K^* component in each δm bin. The dashed lines indicate the sum of all backgrounds.

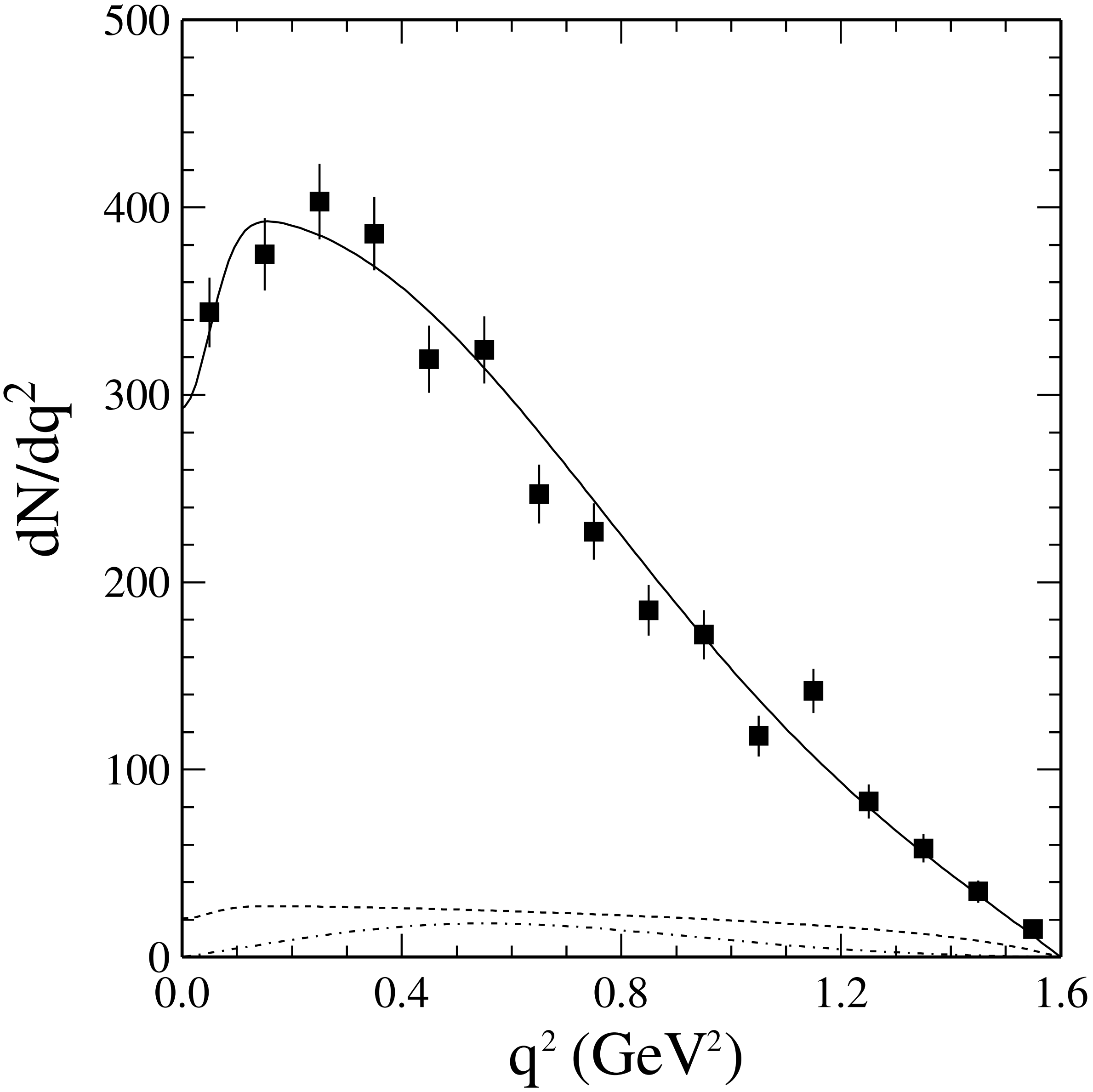

FIG. 4. The q^2 spectrum for the $D^0 \to K^-\ell^+\nu$ sample. The solid curve is the best fit. The dashed line represents the combinatorial background and the dotted line is the contribution from $K^*\ell\nu$ decays.